



# Multi-decadal changes in the South China Sea mixed layer salinity

Lili Zeng<sup>1,3</sup> · Eric P. Chassignet<sup>2</sup> · Xiaobiao Xu<sup>2</sup> · Dongxiao Wang<sup>1,4</sup>

Received: 16 June 2020 / Accepted: 2 March 2021

© The Author(s), under exclusive licence to Springer-Verlag GmbH Germany, part of Springer Nature 2021

## Abstract

A recently assembled South China Sea Physical Oceanographic Dataset provides the first observational evidence for mixed layer salinity changes in the South China Sea from 1960 to 2015. During this period, the mixed layer waters freshened by 0.22 psu. The mixed layer salinity variability is found to be in sync with the Pacific Decadal Oscillation; it freshened in the 1960s, started to salinify in 1974, freshened again from 1993, and then salinified once again from 2012, with linear trends of  $-0.019$ ,  $0.020$ , and  $-0.024$  psu/year, respectively. A box-average salinity budget analysis shows that the surface forcing, horizontal advection, and vertical entrainment terms together can, to a large degree, explain the observed trend in mixed layer salinity. The mixed layer freshening is driven by weakened surface fresh water loss and saline water transport, while salinification is associated with enhanced surface freshwater loss and salt transport through the Luzon Strait. The long-term mixed layer salinity changes affect the stratification, inducing a thinner mixed layer and stronger barrier layer during freshening periods that favor stronger regional ocean–atmosphere interaction.

**Keywords** South China Sea · Mixed layer salinity · Long-term variability

## 1 Introduction

The global water cycle is a key element of the climate system, yet it is poorly understood primarily because most of it occurs over the vast and under-sampled oceans (Schmitt 1995, 2008). There is, however, ample evidence from salinity observations and numerical results from climate models indicating that the water cycle has changed over the past six decades (Wong et al. 1999; Munk 2003) and that it has intensified (Durack et al. 2012).

Ocean salinity is globally conserved and quantification of its variability is essential to understanding the linkages between the water cycle and climate change (Curry et al. 2003; Boyer et al. 2005; Schmitt and Blair 2015). Salinity measurements are used to diagnose changes in important components of the earth climate dynamics, such as surface freshwater flux, freshwater transport, and ocean mixing (Lukas and Lindstrom 1991; Wijffels et al. 1992; Dickson et al 2002; Li et al. 2016a, b). Robust and spatially coherent trends in salinity are found in the global ocean, where surface salinity increases are observed in evaporation-dominated regions and decreases are observed in precipitation-dominated regions (Durack and Wijffels 2010; Skliris et al. 2014).

An abundance of historical records combined with recent observations from various programs have been used to document salinity changes throughout the globe. Long hydrographic records show that the salinity changes in the North Atlantic can be associated with significant changes in the North Atlantic Oscillation index (Dickson et al. 2002; Häkkinen 2002; Curry et al. 2003; Holliday et al. 2008; Sarafanov et al. 2008). Combined surface measurements document Pacific Decadal Oscillation (PDO)-like signals in sea surface salinity in the tropical Pacific (Delcroix et al. 2007; Du et al. 2015; Nan et al. 2015). Recent observations in the

✉ Lili Zeng  
zenglili@scsio.ac.cn

✉ Dongxiao Wang  
dxwang@scsio.ac.cn

<sup>1</sup> State Key Laboratory of Tropical Oceanography (LTO), South China Sea Institute of Oceanology, Chinese Academy of Sciences, Guangzhou 510301, China

<sup>2</sup> Center for Ocean-Atmospheric Prediction Studies, Florida State University, Tallahassee, FL 32306, USA

<sup>3</sup> Southern Marine Science and Engineering Guangdong Laboratory (Guangzhou), Guangzhou 511458, China

<sup>4</sup> School of Marine Sciences, Sun Yat-Sen University, Guangzhou 510275, China

Southern Indian Ocean show a fast freshening since 1995 with a particularly striking acceleration since 2006 (Anilkumar et al. 2015; Menezes et al. 2017; Du et al. 2015).

The South China Sea (SCS) is the largest tropical marginal sea and has one of the lowest average surface salinity levels ( $\sim 33$  psu) (Yang et al. 2019; Zeng et al. 2014). It is located in the Indo-Pacific Ocean, identified by Durack et al. (2012) as one of the areas that experienced the most significant freshening during the 1950–2000 period. The temperature and salinity variations and controlling factors in the SCS are remarkably different from those in the open ocean. The South China Sea Throughflow (SCSTF) connects the Pacific and Indian Oceans, acts as an oceanic bridge, and strongly affects the heat and freshwater budgets in the SCS (Qu et al. 2006; Wang et al. 2006; Liu et al. 2012a, b; Gordon et al. 2012). The SCSTF consists of inflow through the Luzon Strait and outflows through the Karimata, Mindoro, and Taiwan Straits, respectively (Fig. 1). The large quantity of saline water brought through the Luzon Strait by the SCSTF can contribute as much salinity variations in the SCS as the local freshwater flux.

Due to the limited amount of observations, only a few studies have focused on salinity changes in the SCS and most of the attention has been on the northern SCS (Liu et al. 2012a, b; Nan et al. 2013, 2016; Zhao et al. 2014; Zeng et al. 2014, 2016a, b). Nan et al. (2013, 2016) showed that the freshening in the northeastern SCS in the 1990s and 2000s was associated with a weakening trend of the Kuroshio intrusion. Zeng et al. (2014) also found that the extreme freshening event in the northern SCS during 2012 was caused by a weak Kuroshio intrusion. Year 2012 is also when a 20-year freshening trend was reversed (Zeng et al. 2018). Decadal variability has been documented for subsurface salinity in the northern SCS during 1960 and 2012 (Zeng et al. 2016a). Finally, Liu et al. (2012a, b) and Zhao et al. (2014) showed decadal changes in intermediate waters along  $18^\circ$  N in the northern basin (Liu et al. 2012a, b; Zhao et al. 2014). However, very little is actually known about the decadal and long-term variability for the SCS as a whole.

In this paper, we analyze a recent observational dataset with the aim of (1) understanding the decadal and longer-term upper salinity changes in the SCS over the past six decades and (2) assessing the factors that contribute to

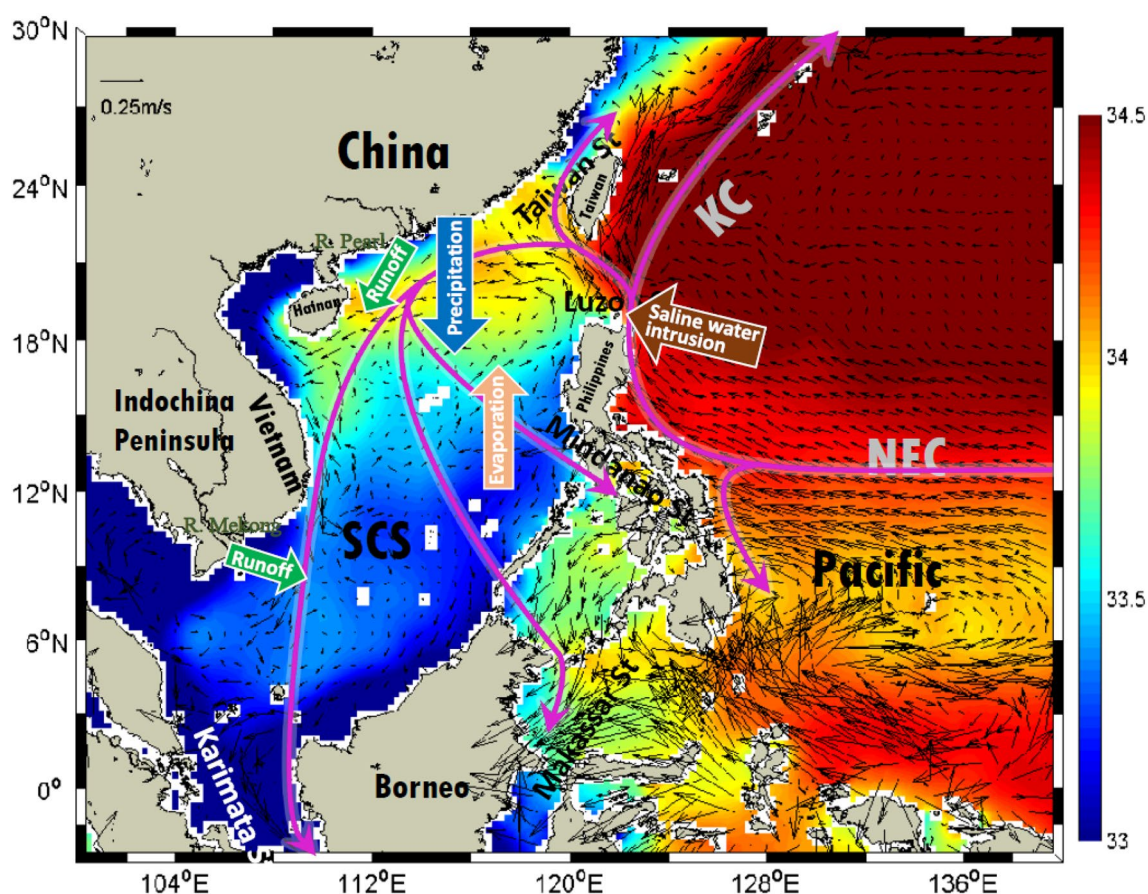


**Fig. 1** WOA mean surface salinity and OSCAR mean surface currents. Major currents in the SCS and adjacent waters are from Qu et al. (2006) and Hu et al. (2015), indicated by magenta lines. SCS South China Sea, NEC North Equatorial Current, KC Kuroshio Current

these changes using a box-average mixed layer salinity budget analysis. The paper is organized as follows. The data and variables used to compute the budget are presented in Sect. 2. The observed changes in salinity over the period 1960–2015 and the possible influence of the PDO are presented in Sect. 3. In Sect. 4, the box-average mixed layer salinity budget and the possible factors controlling variations in the mixed layer salinity are documented. Finally, conclusion and discussions are given in Sect. 5.

## 2 Data and variables

### 2.1 In situ observational dataset

The South China Sea Physical Oceanographic Dataset (SCSPOD14) consists of validated in situ observations collected from the World Ocean Database 2009 (WOD09), Argo floats, and the South China Sea Institute of Oceanology (SCSIO) measurements for the period 1919–2014 (Zeng et al. 2016b). This dataset has been updated by adding quality-controlled Argo float and SCSIO cruise measurements from 2015 (hereafter, SCSPOD15). Details of the data sampling characteristics, processing method, and quality control of this dataset can be found in Zeng et al. (2016b). We focus on the 1960–2015 period because the spatial and temporal coverage of the observations is dense enough to document variability. Overall, 34,485 records located deeper than 50 m within the well-sampled region (107–121° E, 3–23° N) are used for the analysis (Fig. 2a). The spatial distributions of the observations as a function of longitude and latitude are shown in Fig. 2b, c, as well as their sources: WOD09, Argo, and SCSIO. There are no salinity observations in SCSPOD15 for the year 2003, and several years in the mid-1960s have few observations. The interior basin (110–120° E) and northern basin (15–23° N) are sampled quite well with only a few years of poor data coverage. However, in the region west of 110° E and south of 15° N, the sampling is quite sparse between mid-1990s

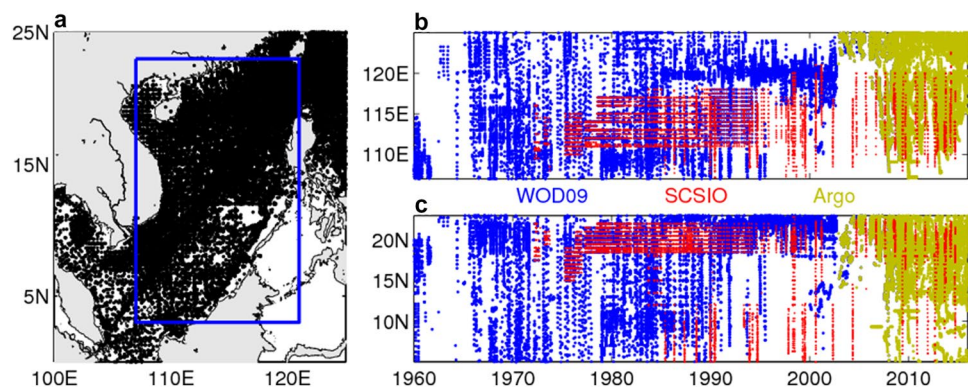
and mid-2000s. The mixed layer depth, mixed layer salinity, and barrier layer thickness are calculated for each profile as described in detail by Zeng et al. (2016b).

### 2.2 Variables

To assess the impact of the air-sea freshwater flux (i.e., evaporation–precipitation–river runoff,  $E-P-R$ , positive freshwater flux indicates loss of freshwater from the ocean), we use the evaporation data from the Objectively Analyzed air–sea Fluxes version 3 (OAFlux; Yu and Weller 2007) together with four precipitation products: the Precipitation Reconstruction (PREC; Chen et al. 2002), the National Centers for Environmental Prediction’s Climate Prediction Center (CPC; Chen et al. 2002), the Global Precipitation Climatology Project version 2.3 (GPCP; Adler et al. 2003), and the Tropical Rainfall Measuring Mission 3B43 (TRMM; Huffman et al. 2007). The four net freshwater  $E-P$  flux datasets are hereafter referred to as PRECflux, CPCflux, GPCPflux, and TRMMflux, respectively. The Mekong and Pearl river runoffs are estimated from the river-basin-integrated precipitation as in Zeng et al. (2014).

To assess the impact of the horizontal salt transport, ocean currents from several products are used. They include the Simple Ocean Data Assimilation (SODA version 2.2.4,  $1/2^\circ$  spatial resolution) monthly reanalysis data from 1960 to 2012 (Carton and Giese 2008), the National Centers for Environmental Prediction (NCEP) Global Ocean Data Assimilation System (GODAS,  $0.333^\circ$  latitude and  $1^\circ$  longitude spatial resolution) monthly reanalysis data from 1980 to 2012 (Huang et al. 2010), daily reanalysis data from 1993 to 2015 from the Hybrid Coordinate Ocean Model (HYCOM) data assimilative system GOFS 3.1 (HYCOM + NCODA Global  $1/12^\circ$  Analysis, Chassignet et al. 2009; Metzger et al. 2014), monthly outputs from the quasi global OGCM for the Earth Simulator (OFES,  $1/2^\circ$  spatial resolution) hindcast simulation driven by daily mean wind stress of the NCEP/NCAR reanalysis data from 1960 to 2010 (Sasaki et al. 2007), and 3-day mean West Pacific (including the SCS) hindcast data from 1992 to 2015 using the Regional Ocean

**Fig. 2** **a** Spatial distributions of observations from the SCSPOD15 dataset. The blue box represents the study area (SCS; 107–121° E, 3–23° N). **b** Longitude–time sections for the 3–23° N band of observations. **c** Latitude–time sections for the 107–121° E band of observations. The three data sources are marked by different colors: WOD09 (blue dots), SCSIO (red dots), and Argo (green dots)



Modeling Systems (ROMS,  $1/8^\circ$  spatial resolution; Xiu et al. 2010). These reanalysis and model datasets all show similar multi-decadal variations of upper layer salinity in the SCS. Finally, to assess the vertical entrainment, we use NCEP wind stress, OFES vertical velocity outputs, and mixed layer depth calculated from SCSPD15 profiles.

### 3 Observed features

#### 3.1 Salinity change between 1960 and 2015 (56 years)

We start by first looking at the long-term salinity change in the upper 250 m from 1960 to 2015 (56 years). The longitudinally and latitudinally averaged salinity changes in the SCS for the upper 250 m were obtained using SCSPD15 and its variability are displayed in Fig. 3a, b. Note that shallow regions less than 250 m are not include in the average. Between 1960 and 2015, the salinity in the upper 50 m is marked by a significant long-term decrease of 0.22 psu in salinity (Fig. 3a), with an averaged trend of  $-0.20$  psu/50 year. This freshening trend can extend as far down as 100 m in the western SCS. In the east, the freshening near the Luzon Strait is even deeper extending as far down as 250 m. The freshening in the upper 100 m is also robust in the latitudinally averaged section, especially in the northern and central basin (Fig. 3b). Below the freshening upper layer, both longitudinally and latitudinally averaged salinity changes show an apparent subsurface salinification beneath 100 m in the central basin (Fig. 3a, b). Figure 3c gives the basin-wide averaged profile of salinity

changes from 1960 to 2015 in the SCS. The profile shows that the SCS experienced a significant freshening in the top 100 m and weak salinification in the subsurface layers (Fig. 3c). Regions where the freshening magnitude exceeds 0.20 psu/50 year are limited to the mixed layer waters.

The linear trends in mixed layer salinity are calculated on  $2^\circ \times 2^\circ$  bins and are displayed in Fig. 4. The crosses indicate the bins in which the computations of trends are not reliable using a Mann–Kendall test. Overall, the mixed layer salinity

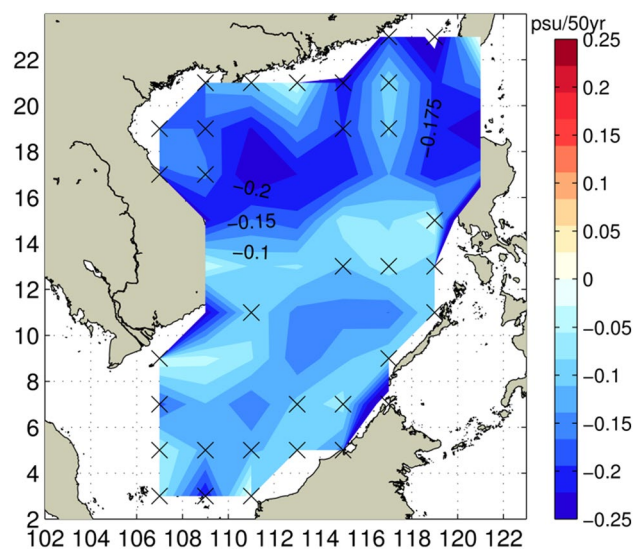
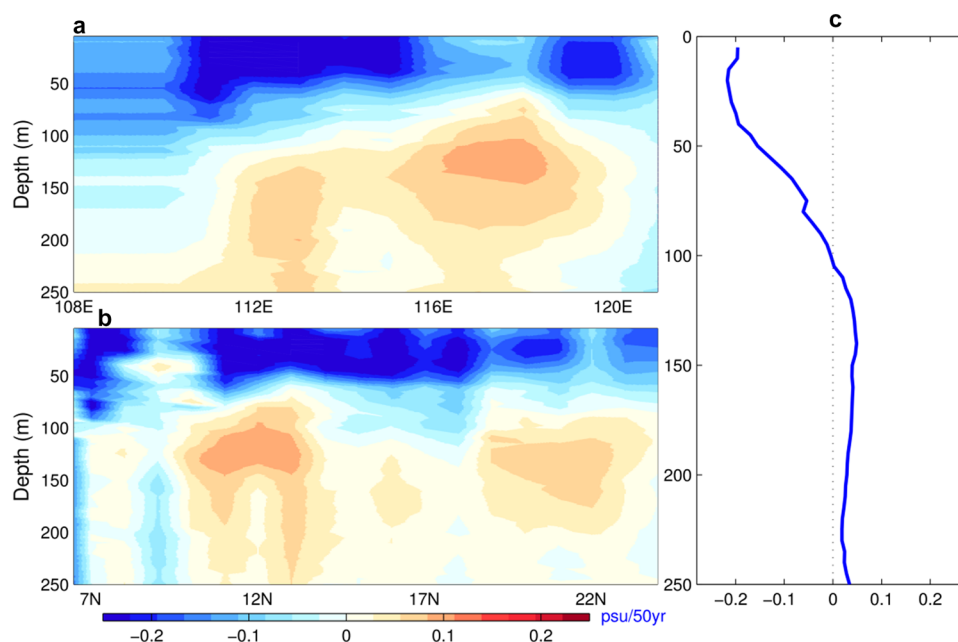


**Fig. 4** The linear trends in the mixed layer salinity calculated within each  $2^\circ \times 2^\circ$  bins in the SCS. The cross delimits bins where the calculations of trends are not reliable in Mann–Kendall test. In order to compare with the trend identified by Durack et al. (2012), the unit is psu/50 yr in this figure

**Fig. 3** Vertical distributions of upper salinity change (psu/year) from 1960 to 2015 in the SCS (basin area is defined as the region shown in Fig. 2a). **a** Longitudinally average, **b** Latitudinally average, and **c** basin-wide average for the SCS. In order to compare with the trend identified by Durack et al. (2012), the unit is psu/50 yr in this figure



in the SCS has been decreasing over the past 56 years, with an averaged trend of  $-0.15$  psu/50 year (or  $-0.003$  psu/year). In the northeastern region, the long-term freshening trend is about  $-0.175$  psu/50 year. This trend is comparable to the value east of the Luzon Strait reported by Durack et al. (2012), i.e.,  $-0.15$  to  $-0.20$  psu over a 50-year period (1950–2000). The freshening trend is weaker in the southern part of the basin than in the northern basin. Note that we cannot clearly state how much of the spatial pattern in the southern basin is due to less observational data distribution. But at the present stage, it will provide valuable observational spatial salinity changing information in the SCS.

### 3.2 Decadal variability

The decrease in mixed layer salinity between 1960 and 2015 is not necessarily linear; freshening during one time period could alternate with salinification during another. To explore the decadal variability, we first show in Fig. 5 the

temperature-salinity ( $T-S$ ) diagram averaged basin-wide for each of the six decades. These  $T-S$  curves are an effective way to distinguish freshening or salinification periods (decades) from the climatological mean conditions. They show that the SCS has experienced significant decadal variability over the past six decades. The upper ocean salinity is highest in the 1990s and lowest in the 2010s. The great salinification of the 1990s also occurred in the Atlantic, tropical Pacific, and Indian Ocean (Curry et al. 2003; Delcroix et al. 2007; Skliris et al. 2014). These decadal differences can be seen in all of the datasets (WOD09, SCSIO, and Argo) that comprise SCSP0D15. Different datasets show important similarities in the decadal changes over the past 60 years. Except that the saltier water brought by Argo floats from the western Pacific cause the difference between Argo and SCSIO in 2010s in certain degree (Fig. 5c, d).

To further illustrate the variability of the salinity in the SCS, in Fig. 6a we plot yearly variations of basin-wide averaged salinity for the upper 250 m from 1960 to 2015. The

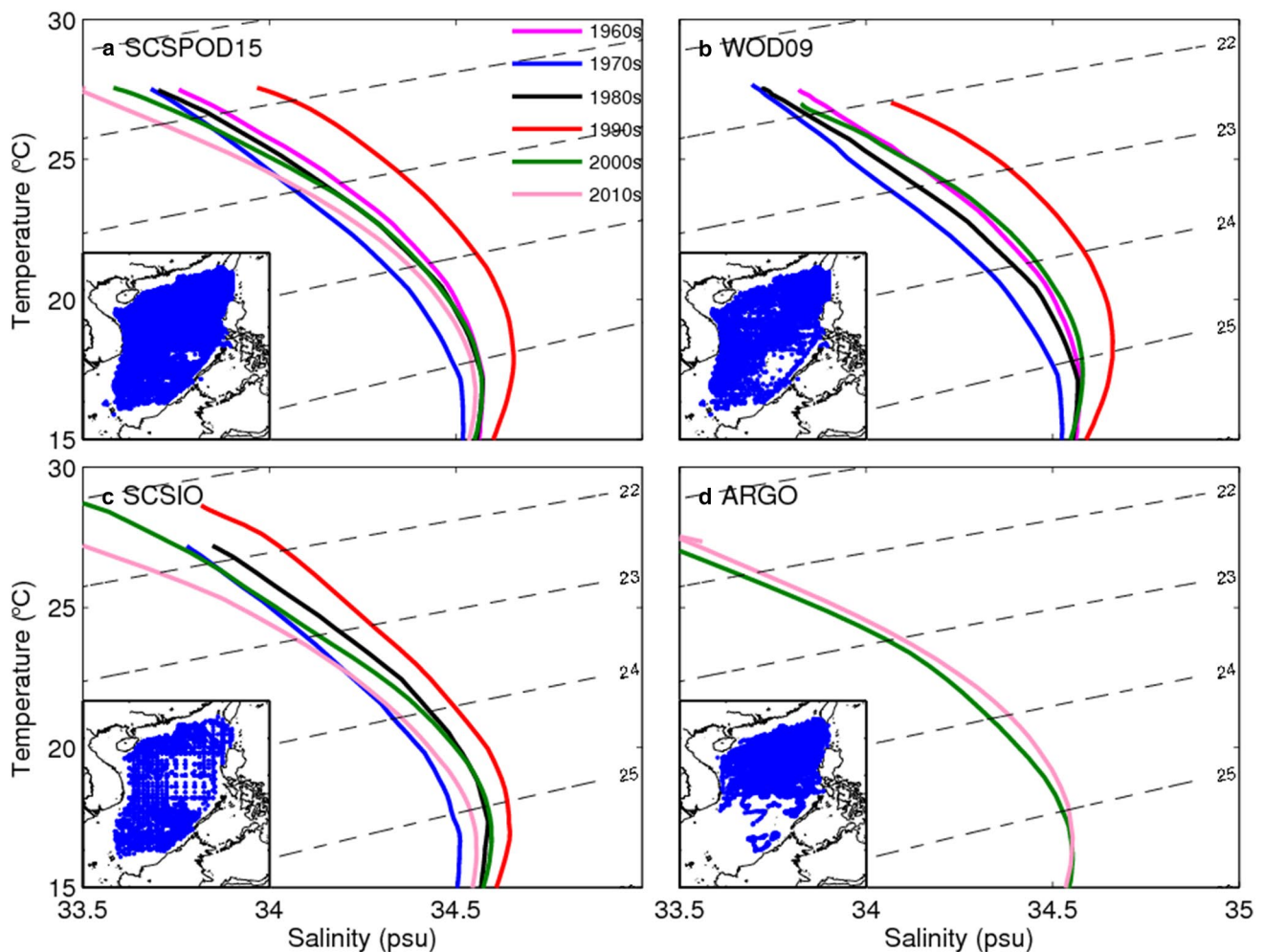
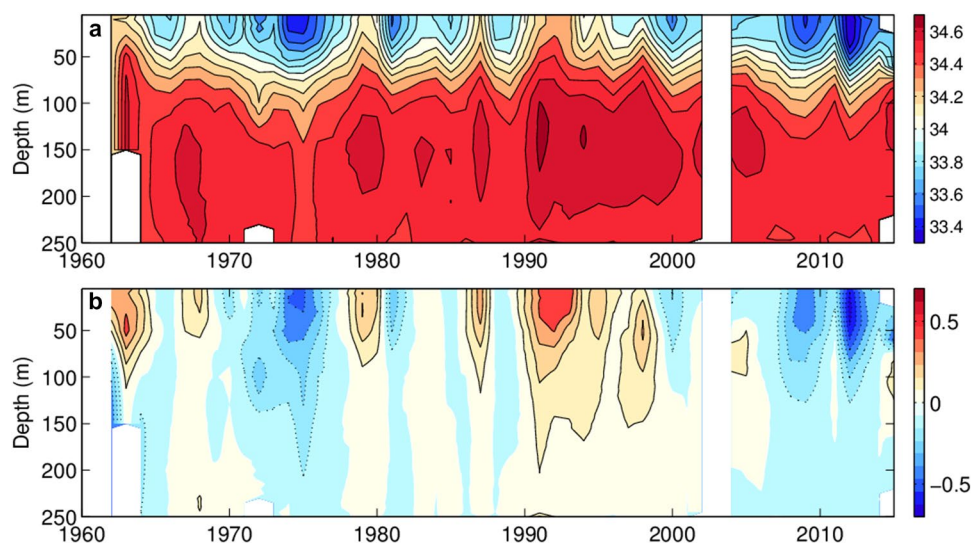


**Fig. 5** Decadal mean  $T-S$  curves from 1960 to 2015 in the upper SCS (1960s: magenta; 1970s: blue; 1980s: black; 1990s: red; 2000s: green; 2010s: pink) based on, **a** SCSP0D15; **b** WOD09; **c** SCSIO; **d** Argo

**Fig. 6** Time-depth sections of basin-wide averaged yearly mean **a** salinity, and **b** salinity anomalies (take off the temporal averaged yearly time-depth section, positive salinity anomaly: red; negative salinity anomaly: blue) in the upper SCS

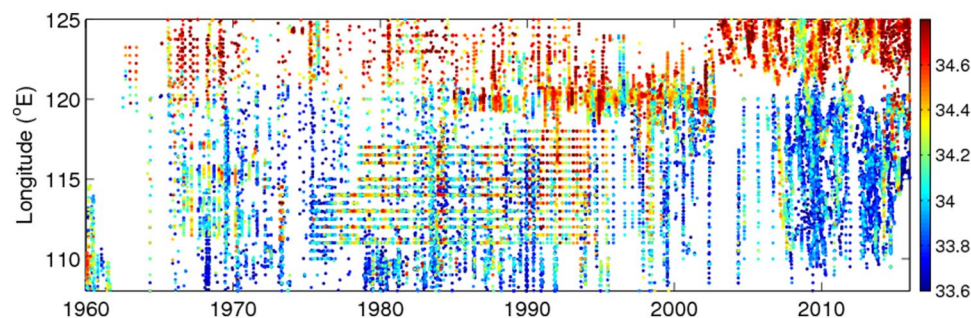


upper ocean started to freshen in the 1960s and continued through the mid-1980s. This was followed by a short salinification period in the late 1970s, then freshening again until the mid-1990s. Significant freshening occurred yet again in the 2010s. This variability, which can be as high as 0.4 psu, is clearly visible in the salinity anomaly plot (Fig. 6b), with phases of high salinity in the 1960s and mid-1990s and low salinity in the mid-1970s and the 2010s. The salinity anomalies can extend down from the surface to about 200 m, but the highest anomalies with amplitude of up to 0.4 psu are mostly confined to the mixed layer. We therefore now focus on the mixed layer salinity variability.

### 3.3 Mixed layer salinity variability

Figure 7 shows longitude–time sections of mixed layer salinity from 1960 to 2015 averaged between 3° N and 23° N. There is a striking difference between the SCS and Pacific waters east of 121° E. The mixed layer salinity in the SCS is significantly lower than that of Pacific waters. As discussed in the previous section, the mixed layer salinity underwent freshening in the 1970s, salinification during the 1980s and 1990s (~0.4 psu), and then freshening again. The lowest salinity was recorded in 2012 (Zeng et al. 2014).

**Fig. 7** Longitude–time sections of mixed layer salinity (color, psu) for the 3–23° N band from 1960 to 2015 in the SCS



This is summarized by Fig. 8, which shows the temporal evolution of the basin-wide mixed layer salinity, including the one standard errors. The error bar is estimated as the standard error of all mixed layer salinity values for a given calendar year. The 7-year band pass time series (in blue) can be divided into four periods separated by three mixed layer salinity minima and maxima: 1974 (the secondary minimum mixed layer salinity), 1993 (the maximum mixed layer salinity), and 2012 (the minimum mixed layer salinity). The observed change in mixed layer salinity was first a decrease of about  $-0.4$  psu during 1960–1974. The mixed layer salinity then increased by  $\sim 0.6$  psu between 1974 and 1993, followed by a sharp decrease of  $\sim 0.7$  psu between 1993 and 2012. It increased again after 2012. The corresponding linear trends are  $-0.020$ ,  $0.019$ , and  $-0.024$  psu/year, about one order of magnitude higher than the 56-year long-term trend ( $-0.004$  psu/year). All trends reported here are statistically significant according to the *t*-test. The salinity change rates in the mixed layer are about two to three times higher than those reported for the subsurface layer by Zeng et al (2016a).

To explore the regional differences in mixed layer salinity variability, yearly variations in the mixed layer salinity anomaly averaged over six well-sampled regions are shown

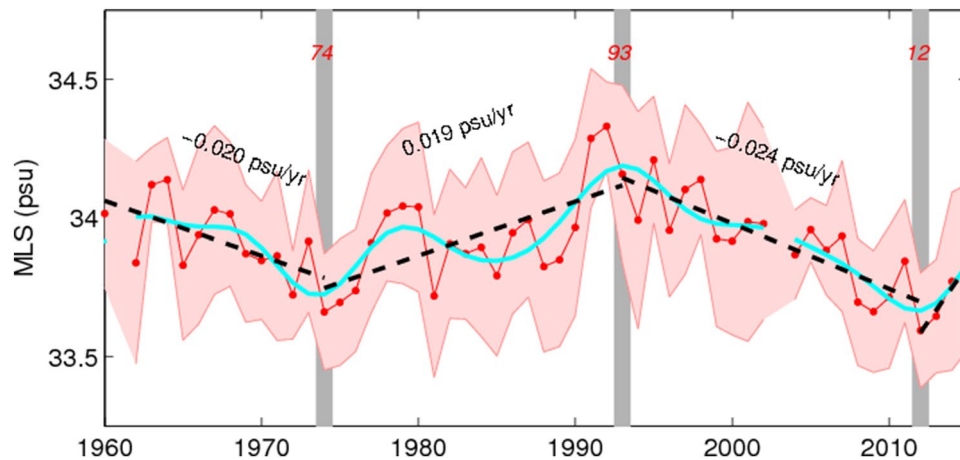


**Fig. 8** Time series of average yearly basin-wide mixed layer salinity from 1960 to 2015 in the SCS. Shading (light red) indicates error bars. The error bar is estimated as the standard error of all mixed layer salinity values for a given calendar year. The low-frequency

curve (blue) represents the seven-year filtered values used to highlight long-term changes. The dashed line represents the linear least squares fit of the yearly values used to quantify linear trends (psu/year). The gray shaded areas indicate turning points in 1974, 1993, and 2012

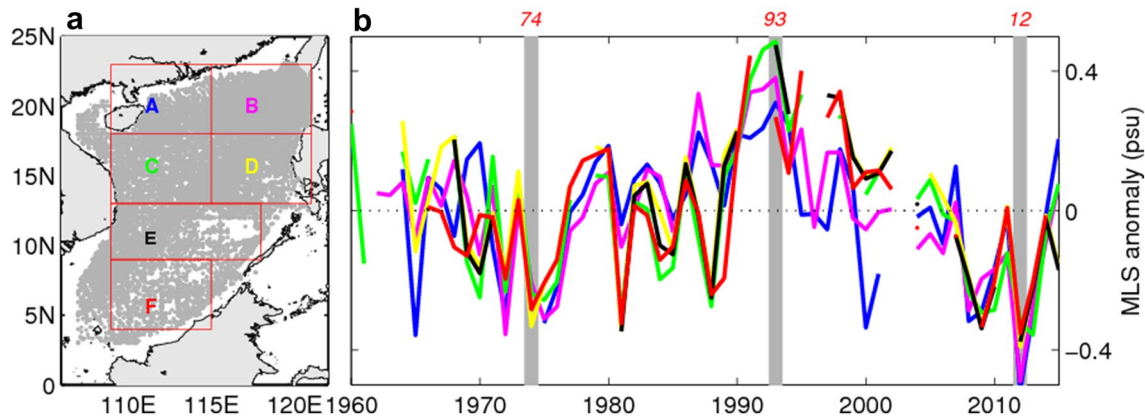


**Fig. 9** **a** Spatial distributions of selected SCSPD15 observations in the study area (107–121° E, 3–23° N) and six selected areas (boxes) used for spatial averages. **B** Time series of yearly mixed layer salinity anomalies averaged in the six areas (take off the box-averaged

yearly mixed layer salinity) from 1960 to 2015 in the SCS indicated by boxes in **a**. The gray shaded areas indicate turning points in 1974, 1993, and 2012

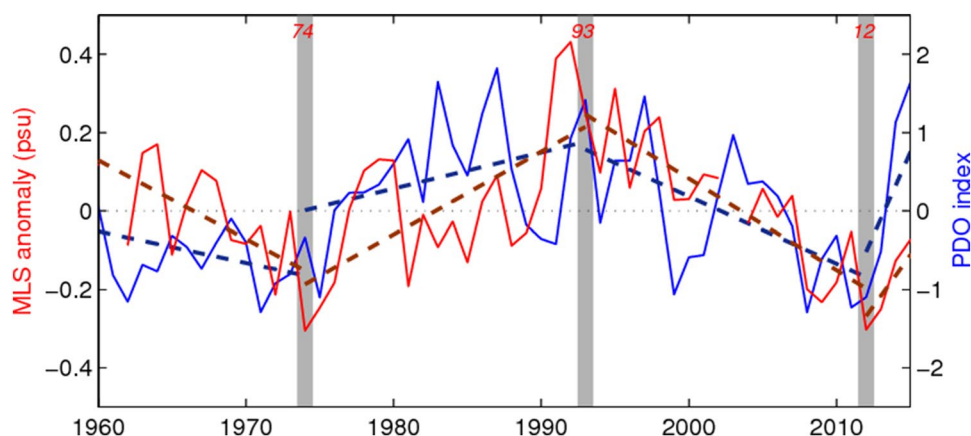
in Fig. 9. The decadal timescale variability is similar for each region with a salinification period that is slightly more noticeable in the northern basin than in the southern basin.

### 3.4 Mixed layer salinity variability and the PDO

As the largest marginal sea in the northwest Pacific Ocean, the climate and environment of the SCS are strongly influenced by the PDO. For example, a coral geochemistry record in the northern SCS was reported to be significantly correlated with the PDO index over the last century (Deng et al. 2013). In Fig. 10, we superimpose the mixed layer salinity anomaly on the PDO index and find that there is a reasonably good agreement between the two curves.

The correlation between yearly mean mixed layer salinities and the PDO index is 0.45 at the 95% confidence level. Their correlation is much higher after the 1990s (0.52) than prior (0.19). The freshening periods generally coincide with a declining stage of the PDO index, while the salinification periods are associated with an ascending stage. The largest change in PDO index and mixed layer salinity occurs after 2012 when both the mixed layer salinity and the PDO index rise quickly. This salinification from late 2012 occurs when the phase of PDO switches from negative to positive has been discussed in detail in our previous work (Zeng et al. 2018).

**Fig. 10** Time series of yearly PDO index (blue) and mixed layer salinity anomaly (take off the basin-averaged yearly mixed layer salinity, red) in the SCS from 1960 to 2015. The gray shaded areas indicate turning points in 1974, 1993, and 2012. The blue and red dashed line represents the linear least squares fit of the yearly values used to quantify linear trends for PDO and mixed layer salinity anomaly, respectively



#### 4 Factors controlling variations in the mixed layer salinity

What are the reasons for the salinification and freshening in the SCS mixed layer salinity? In general, factors that can cause the mixed layer salinity changes include (a) net air-sea freshwater flux, (b) the Luzon Strait transport induced horizontal salt advection, and (c) vertical entrainment and small-scale mixing processes. In this section, we focus on the change in the surface freshwater flux and the surface current during salinification/freshening periods (4.1); we then provide a more quantitative assessment for each factor that contributes to the observed salinity change (4.2 and 4.3).

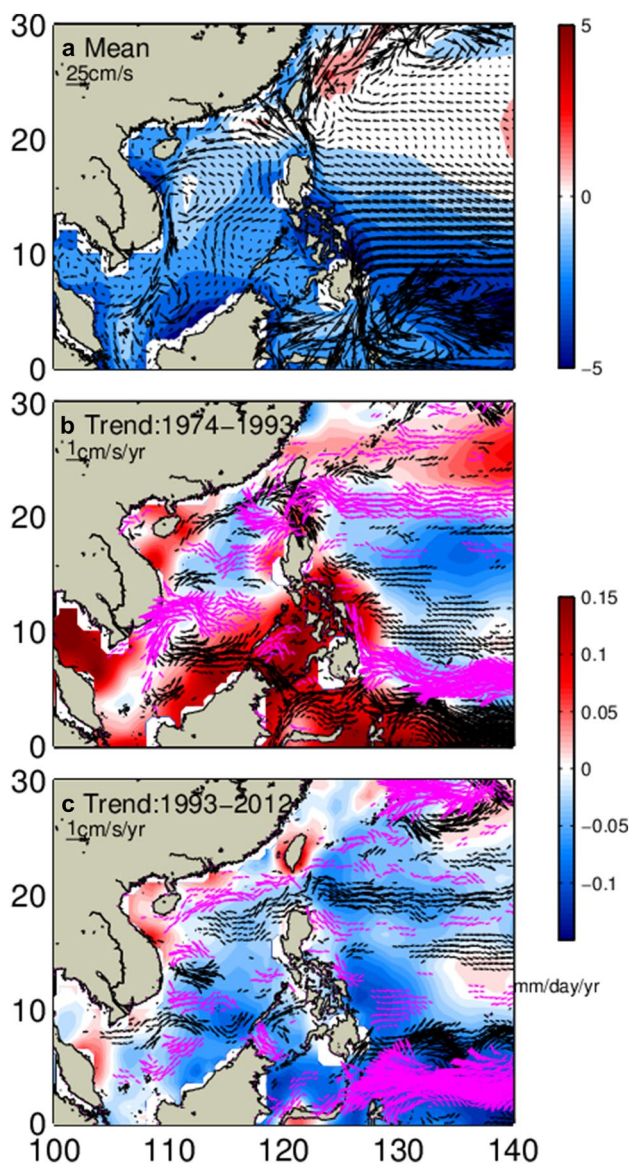
##### 4.1 Dry/wet conditions during salinification/freshening periods

Figure 11a displays the spatial distribution of the long-term (1960–2015) mean net surface freshwater flux (color shading) based on the GPCP and mixed layer circulation (vectors) based on the OFES model simulation. GPCPflux dataset and the OFES surface velocities are shown here because of their good spatio-temporal coverage in the SCS. Over the 56-year period (Fig. 11a), evaporation is lower than precipitation in the SCS, except to the southwest of Taiwan. There is also a clear signature of the Kuroshio intrusion across the Luzon Strait in the SCS circulation.

Figures 11b, c show the change in the surface freshwater flux and the mixed layer current for a salinification period (1974–1993) and a freshening period (1993–2012). During the 1974–1993 salinification period (Fig. 11b), the increasing trend of freshwater loss dominated almost everywhere, except for the central northern SCS where the freshwater flux was negative. In the surface circulation, there is an anomalous westward flow trend east of the Luzon Strait (red vectors, Fig. 11b) that, according to Yu and Qu (2013), is an indication of a northward shift of the North Equatorial Current (NEC) bifurcation, suggesting a

stronger Kuroshio intrusion or larger Luzon Strait transport. During the 1993–2012 freshening period (Fig. 11c), the net freshwater flux and ocean current distribution were opposite to that of the 1974–1993 salinification period. There is a decreasing trend of net freshwater loss across almost the entire basin and the eastward flow trend east of the Luzon Strait was unfavorable for Kuroshio intrusion (black vectors, Fig. 11c). In summary, the trends of enhanced (decreased) freshwater loss and Luzon Strait transport provided salinification (freshening) conditions during a salinification (freshening) period.

Previous studies have shown that the PDO has an important influence on Asian monsoon and monsoon precipitation. The PDO can either strengthen or weaken the Walker circulation over the Indo-Pacific Ocean depending on the phase of the PDO (Krishnamurthy and Krishnamurthy 2014). For the SCS, during positive PDO phases the descending motion of the Walker circulation leads to drought conditions over the basin, while during negative phases the ascending motion brings heavy rainfall to the SCS. The net freshwater loss is generally above average during the ascent PDO stage and below average during the declining PDO stage, with exceptions occurring during the mid-1990s and 2000s (Fig. 12). Du et al. (2015) also reported a reduction in freshwater loss in the southeastern tropical Indian Ocean starting from the mid-1990s due to intensified Walker circulation. Yu and Qu (2013) found a significant imprint of the PDO on decadal SCSTF variability. They indicated that during positive PDO phases, the NEC bifurcation shifts northward and is responsible for the southward intrusion of the Aleutian low, leading to a weaker Kuroshio and stronger SCSTF in the upper 750 m. As shown in Fig. 12, we find that the Luzon Strait transport integrated within the mixed layer is also closely related to the PDO index and, in the previous section, we showed that the averaged SCS mixed layer salinity variations are in sync with the PDO.



**Fig. 11** **a** Long-term mean GPCP freshwater flux ( $E-P$ , shading, unit: mm/d) and OFES mixed layer circulation (vectors, unit: cm/s). **b** Linear trend of GPCP freshwater flux (shading, unit: mm/d/yr) and OFES circulation from 1974 to 1993 (magenta vectors: westerly currents; black vectors: easterly currents; unit: cm/s/yr). **c** Same as **b**, but for the period 1993–2012

## 4.2 Box-average mixed layer salinity budget

In this section, we address whether the contribution of freshwater flux and Luzon Strait salt transport changes can fully account for the observed mixed layer salinity variations. In order to quantify the factors affecting the mixed layer salinity in the SCS, we perform a mixed layer salinity budget:

$$\underbrace{\frac{\partial S_m}{\partial t}}_{\text{Salinity tendency}} = \underbrace{\frac{S_0 \cdot (E - P - R) \cdot A_{SCS}}{V_{SCS}}}_{\text{Surface forcing}} + \underbrace{\frac{T_{in} \cdot \Delta S_{in}}{V_{SCS}} - \frac{T_{out} \cdot \Delta S_{out}}{V_{SCS}}}_{\text{Horizontal advection}} - \underbrace{\frac{\Gamma(w_e) \cdot (S_m - S_b)}{H}}_{\text{Vertical entrainment}} + \varepsilon. \quad (1)$$

From left to right, the terms correspond to mixed layer salinity tendency; surface forcing (loss from ocean defined as positive); horizontal advection term (defined as positive into the SCS), which contain advectations into (second term on right side) and out of (third term) the basin; vertical entrainment; and a residual term, which includes diffusion and other small effects. Here,  $S_m$  is mixed layer salinity,  $S_0$  is the mean sea surface salinity, and  $A_{SCS}$ ,  $H$ , and  $V_{SCS}$  are the surface area, mixed layer depth, and volume of the SCS (111°–121° E, 16°–22° N), respectively.  $E$  is the evaporation,  $P$  is the precipitation, and  $R$  is the river discharge; their net value is the net freshwater flux out of the basin (loss from the ocean is defined as positive).

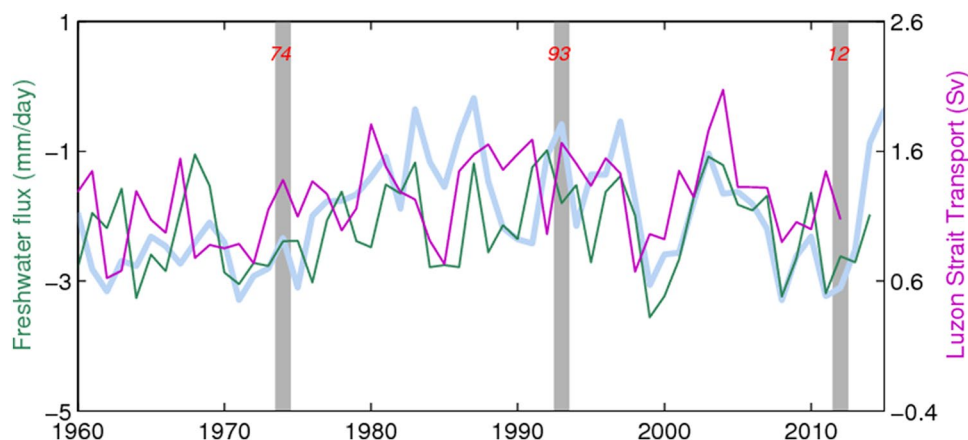
Accurately quantifying the horizontal advection over the entire basin is difficult. For a basin-wide study, the horizontal salinity transport can be represented by two components: inflow and outflow salt transport terms. Here,  $T_{in}$  and  $T_{out}$  are the volume transports into and out of the basin, respectively, and  $\Delta S_{in}$  ( $\Delta S_{out}$ ) is the salinity difference between waters outside the inflow (outflow) straits and waters within the SCS, where a positive transport term means an enhanced salinity effect. As mentioned earlier, the exchange between the SCS and surrounding oceans consists mainly of inflow from the Kuroshio through the Luzon Strait, and outflow primarily through the Mindoro, Karimata, and Taiwan Straits (Yaremchuk et al. 2009). According to Qu et al. (2005), Song (2006) and Nan et al. (2016), the freshwater exports across the outflow straits do not contribute much to the interannual SCS salinity budget, and we therefore did not take into account the freshwater export through the Taiwan, Mindoro and Karimata Straits.

The vertical processes contain vertical Ekman velocity and diapycnal mixing velocity (Michel et al. 2007). Following Michel et al. (2007) and Yu (2015), we have

$$w_e = w_{Ek} + w_m = \frac{\nabla \times \tau}{\rho f} + \left( \frac{\partial H}{\partial t} + \nabla \cdot HU \right), \quad (2)$$

where  $\tau$  denotes wind stress,  $\rho$  the mixed layer density,  $f$  the Coriolis frequency, and  $U$  includes Ekman and geostrophic current. The Ekman velocity  $w_{EK}$  corresponds to the upwelling (downwelling) generated by the convergence (divergence) of the horizontal Ekman transport (Yu 2015). The mixing velocity  $w_m$ , or the mixed layer depth

**Fig. 12** Time series of yearly PREC net freshwater flux ( $E-P$ , green, unit: mm/d), OFES Luzon Strait transport (purple, unit: Sv) and yearly PDO index (light blue, PDO-2 is shown). The gray shaded areas indicate turning points in 1974, 1993, and 2012



tendency, can be influenced by wind, buoyancy, and other thermodynamic processes. In Eq. (1),  $\Gamma$  is the Heaviside function and  $w_e$  is the entrainment velocity at the bottom of the mixed layer;  $S_b$  is defined as the salinity at 20 m below the mixed layer depth (Ren et al. 2011);  $\Gamma$  is used to represent entrainment ( $w_e > 0$ ) and detrainment ( $w_e < 0$ ) to the mixed layer. Only the entrainment of subsurface water affects the mixed layer salinity; detrainment removes mixed layer water but does not modify its salinity (Niiler and Kraus 1977; Michel et al. 2007; Yu 2015).

Thus, we have a simplified expression for the box-average mixed layer salinity variation:

$$\frac{\partial S_m}{\partial t} = \frac{S_0 \cdot (E - P - R) \cdot A_{SCS}}{V_{scs}} + \frac{LST \cdot \Delta S_{lz}}{V_{scs}} - \frac{\Gamma(w_e) \cdot (S_m - S_b)}{H} + \epsilon, \quad (3)$$

where  $\Delta S_{lz}$  is the salinity difference between two sides of the Luzon Strait, the Western Pacific water east of the Luzon Strait ( $S_{WP}$ ) and the SCS ( $S_{SCS}$ ).

### 4.3 Factors controlling the mixed layer salinity variability

To quantify the impact of the uncertainties associated with different data products, we use several datasets (introduced in Sect. 2) for the freshwater flux and the Luzon Strait transport to calculate the contribution of the surface forcing and advection terms to the salinity budget. The temporal evolution of the budget terms are displayed in psu/year in Fig. 13. The surface forcing and the horizontal advection terms dominate and the vertical mixing is smaller by one order of magnitude. The trends for each term during the freshening and salinification periods, using the different datasets, are listed in Table 1.

During the 1960–1974 freshening period, the trends in the surface forcing, advection, and entrainment terms

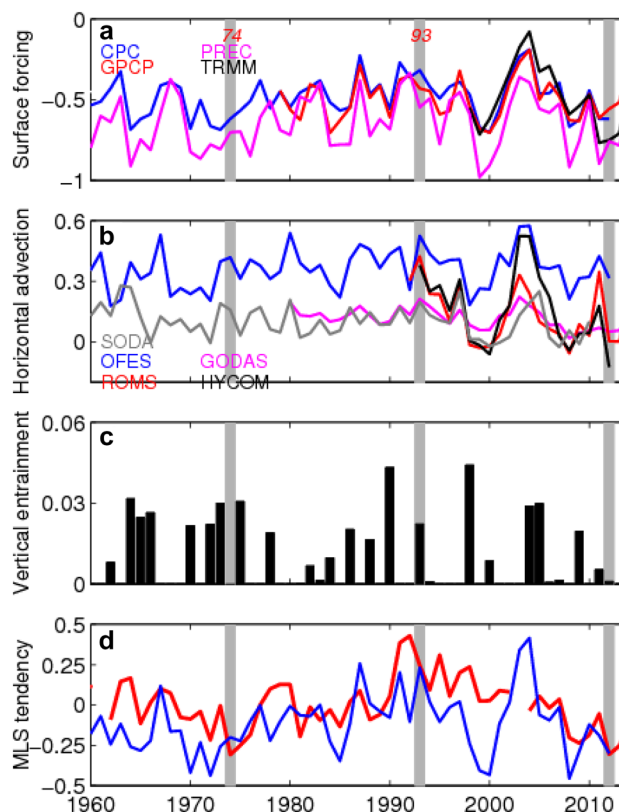


**Fig. 13** Spatial average of each term in Eq. (3) for the SCS (unit: psu/year). **A** Net freshwater flux term (CPCflux: blue; PRECflux: magenta; GPCPflux: red; TRMMflux: black). **B** Luzon Strait transport induced horizontal advection term (SODAadv: gray; OFESadv: blue; GODASadv: magenta; ROMSadv: red; HYCOMadv: black). **C** Vertical entrainment term. **D** Mixed layer salinity tendency, and the sum of the freshwater flux, horizontal advection, and vertical entrainment terms

were  $-0.011$ ,  $-0.006$  and  $-0.0003$  psu/year, respectively. Their total contribution was about  $-0.017$  psu/year, roughly equivalent to the change in mixed layer salinity of  $-0.020$  psu/year. This result indicates that



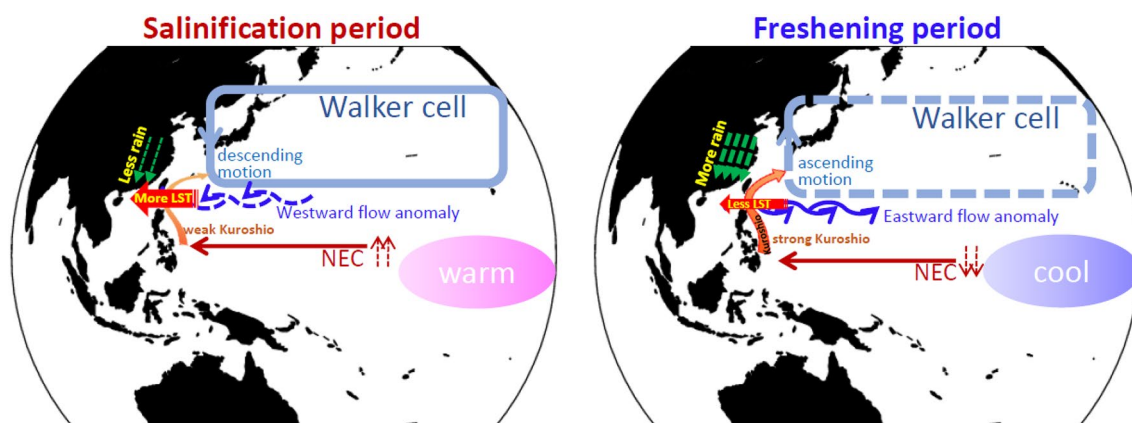


**Fig. 15** Schematic diagram of the **a** salinification and **b** freshening periods in the SCS

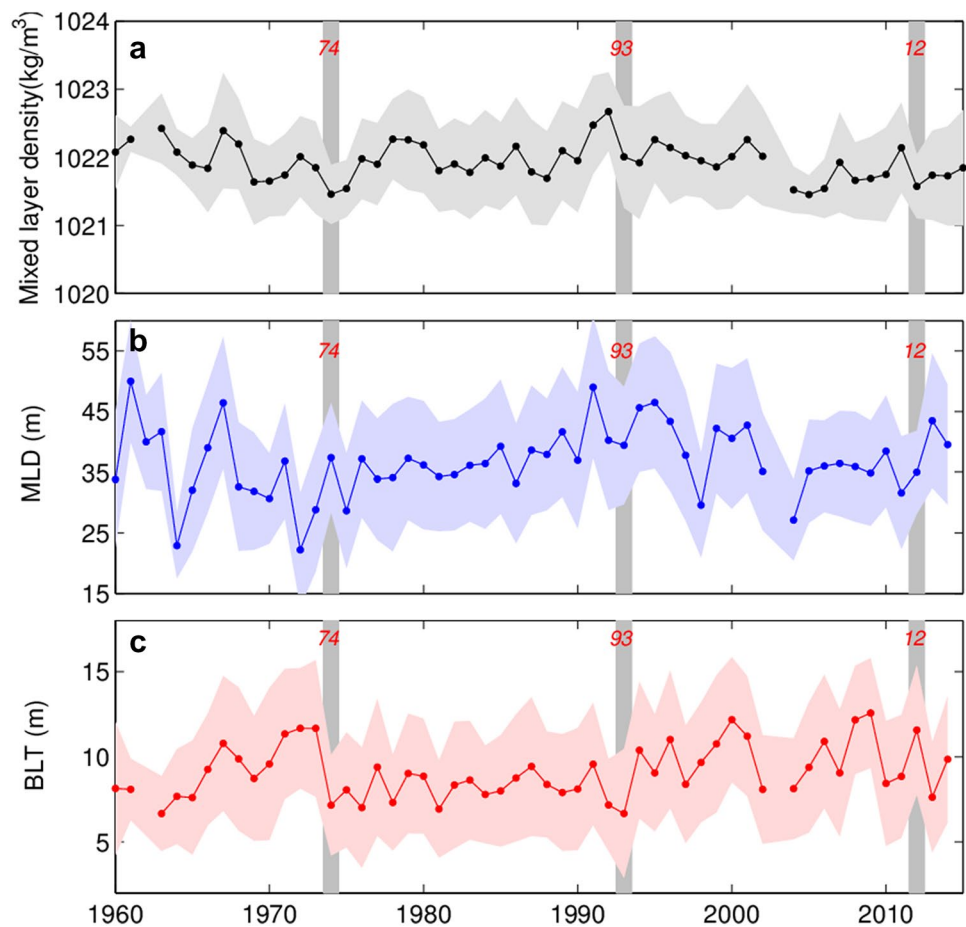
Zeng et al. (2016a, b). We find that the long-term variability in mixed layer salinity is in sync with the PDO. During the ascent (declining) stage of the PDO, the ascending (descending) motion of the Walker circulation leads to flood (drought) conditions over the basin, along with less (more) intrusion of additional saline water by the Luzon Strait transport associated with a stronger (weaker) Kuroshio; this results in freshening (salinification) in the SCS (see schematic Fig. 15).

Although the SCSPOD15 dataset provides unprecedented observational coverage in the SCS, there are still gaps and insufficient and uneven observations in some years. One of the largest uncertainties in the trends assessment comes from the assembled observational dataset. However, because we find that the observed mixed layer salinity variability is in good agreement with the variability derived from a box-average mixed layer salinity budget, we are confident that the trends reported here are representative. The mixed layer salinity budget analysis is then used to quantify the forcing factors controlling long-term changes in mixed layer salinity. The results show that the freshening period is associated with a reduction in both the surface freshwater loss and the Luzon Strait transport advection terms, while salinification is associated with enhanced surface freshwater loss and salt transport through the Luzon Strait. Note that the mixed layer freshening is controlled by equal contributions from the surface forcing and advection terms, while the salinification period is mostly controlled by enhanced surface freshwater loss. While we have assessed the uncertainty by utilizing as many surface forcing products and ocean current outputs as possible (both with and without data assimilation), it is clear that the accuracy of different surface forcing products and the realism of the ocean model current outputs remains an issue. In the simplified salinity budget, the freshwater exports in the Taiwan, Mindoro and Karimata Straits were not taken into account as the freshwater exports across the

outflow straits does not contribute much to the interannual SCS salinity budget (Qu et al. 2005; Song 2006; Nan et al. 2016). However, there are freshwater inputs into the Indonesian Seas that can influence the variability of Indonesian Throughflow (ITF) transport and induce salinity changes in the eastern Indian Ocean (Gordon et al. 2003; Hu and Sprintall 2016, 2017; Lee et al. 2019). Future studies could examine the potential influence of the freshwater outflows of the SCS on the ITF variations and related salinity changes.

Finally, the question as to whether the mixed layer salinity changes (freshening or salinification) can induce significant climate change in the SCS depends on the magnitude of the trends. Sufficiently large salinity changes will modify the ocean stratification and air-sea flux exchanges and, when exceeding a threshold, will impact the SCS thermohaline circulation and the climate (Manabe and Stouffer 1995; Wu et al. 2004). Barreiro et al. (2008) showed that a freshwater input exceeding 0.3 Sv per decade (a model-dependent value) can weaken the thermohaline circulation in the North Atlantic. We are then led to ask what is the threshold that must be exceeded in the SCS to significantly influence its thermohaline circulation? In the SCS, changes in the mixed layer salinity regulate the mixed layer (Fig. 16). The observed mixed layer salinity freshening or salinification trends could constructively contribute to a reduction or enhancement of the mixed layer density (Fig. 16a). The shoaling or deepening of the mixed layer depth generally coincides with a freshening or salinification of the mixed layer salinity (Fig. 16b). Variations in salinity stratification that forms a barrier layer have an important influence on climate (Maes et al. 2002, 2005). For the SCS, there was no significant change in the barrier layer during the salinification, but a shoaling mixed layer depth was associated with a slight increase in the

**Fig. 16** Time series of yearly **a** mixed layer density, **b** mixed layer depth, and **c** BLT averaged in the SCS. Error bars are shown in light shading. The gray shaded areas indicate turning points in 1974, 1993, and 2012



barrier layer during the two freshening periods (Fig. 16c). A combination of the relatively shallow mixed layer and stronger barrier layer during the freshening period could lead to a strengthening of the ocean–atmosphere coupling in the SCS. A realistic climate model and well-designed experiments are needed to answer these questions. Future studies could examine long-term changes in salinity, the threshold for major change, and detailed processes affecting the thermohaline circulation and climate change.

**Acknowledgements** We benefited from several observational datasets and numerical results made freely available, including the SCSPD dataset (<https://figshare.com/s/e5327a334130cd44dc6a>), the OAF-lux evaporation ([ftp://ftp.whoi.edu/pub/science/oaflux/data\\_v3](ftp://ftp.whoi.edu/pub/science/oaflux/data_v3)), the PREC precipitation (<http://www.esrl.noaa.gov/psd/data/gridded/data.prec.html>), the CPC precipitation (<http://apdrc.soest.hawaii.edu/data/data.php>), the GPCP precipitation (<http://www.esrl.noaa.gov/psd/data/gridded/data.gpcp.html>), the TRMM 3B43 precipitation (<http://mirador.gsfc.nasa.gov/cgi-bin/mirador/>), OFES outputs (<http://apdrc.soest.hawaii.edu/data/data.php>), the SODA (<http://sodaserver.tamu.edu/assim/>), the GODAS (<http://www.esrl.noaa.gov/psd/data/gridded/data.godas.html>), and the HYCOM (<http://hycom.org/dataserver/glb-reanalysis>). LZ is supported by the National Natural Science Foundation of

China (nos. 42076209, 41776025, 41776026, 41806035, 41890805, 41676018), Key Special Project for Introduced Talents Team of Southern Marine Science and Engineering Guangdong Laboratory (Guangzhou) (GML2019ZD0306), the Rising Star Foundation of the South China Sea Institute of Oceanology (NHXX2019WL0101) and the Pearl River S&T Nova Program of Guangzhou (201906010051). EPC and XX are supported by the NOAA Climate Program Office MAPP Program (award NA15OAR4310088) and the NSF Physical Oceanography Program (award 1537136).

## References

- Adler RF, Huffman GJ, Chang A, Ferraro R, Xie P, Janowiak J, Rudolf B, Schneider U, Curtis S, Bolvin D, Gruber A, Susskind J, Arkin P, Nelkin E (2003) The version-2 global precipitation climatology project (GPCP) monthly precipitation analysis (1979–present). *J Hydrometeorol* 4:1147–1167
- Anilkumar N, Chacko R, Sabu P, George JV (2015) Freshening of Antarctic bottom water in the Indian Ocean sector of southern ocean. *Deep Sea Res Part II* 118:162–169
- Barreiro M, Fedorov A, Pacanowski R, Philander SG (2008) Abrupt climate changes: how freshening of the northern Atlantic affects

- the thermohaline and wind-driven oceanic circulations. *Annu Rev Earth Planet Sci* 36(36):33–58
- Boyer TP, Levitus S, Antonov JI, Locarnini RA, Garcia HE (2005) Linear trends in salinity for the World Ocean, 1955–1998. *Geophys Res Lett* 32:L01604. <https://doi.org/10.1029/2004GL021791>
- Carton JA, Giese BS (2008) A reanalysis of ocean climate using simple ocean data assimilation (SODA). *Mon Weather Rev* 136:2999–3017
- Chassignet EP, Hurlburt HE, Smedstad OM, Halliwell GR, Hogan PJ, Wallcraft AJ et al (2009) Global ocean prediction with the Hybrid Coordinate Ocean Model (HYCOM). *Oceanography* 22(2):64–75
- Chen MY, Xie PP, Janowiak JE, Arkin PA (2002) Global land precipitation: a 50-yr monthly analysis based on gauge observations. *J Hydrometeorol* 3:249–266
- Curry R, Dickson B, Yashayaev I (2003) A change in the freshwater balance of the Atlantic ocean over the past four decades. *Nature* 426(6968):826–829
- Delcroix T, Cravatte S, McPhaden MJ (2007) Decadal variations and trends in tropical Pacific sea surface salinity since 1970. *J Geophys Res* 112(C3):266–281
- Deng W, Wei G, Xie L, Ke T, Wang Z, Zeng T, Liu Y (2013) Variations in the Pacific Decadal Oscillation since 1853 in a coral record from the northern South China Sea. *J Geophys Res Oceans* 118:2358–2366. <https://doi.org/10.1002/jgrc.20180>
- Dickson B, Yashayaev I, Meincke J, Turrell B, Dye S, Holfort J (2002) Rapid freshening of the deep north Atlantic ocean over the past four decades. *Nature* 416(6883):832–837
- Du Y, Zhang Y, Feng M, Wang T, Zhang N, Wijffels S (2015) Decadal trends of the upper ocean salinity in the tropical Indo-Pacific since mid-1990s. *Sci Rep* 5(16050):2015. <https://doi.org/10.1038/srep16050>
- Durack PJ, Wijffels SE (2010) Fifty-year trends in global ocean salinities and their relationship to broadscale warming. *J Clim* 23:4342–4362
- Durack PJ, Wijffels SE, Matear RJ (2012) Ocean salinities reveal strong global water cycle intensification during 1950 to 2000. *Science* 336(6080):455–458. <https://doi.org/10.1126/science.1212222>
- Gordon AL, Susanto RD, Vranes K (2003) Cool Indonesian throughflow as a consequence of restricted surface layer flow. *Nature* 425(6960):824–828
- Gordon AL, Huber BA, Metzger EJ, Susanto RD, Hurlburt HE, Adi TR (2012) South China Sea throughflow impact on the Indonesian throughflow. *Geophys Res Lett* 39(11):117–128
- Häkkinen S (2002) Freshening of the Labrador Sea surface waters in the 1990s: another great salinity anomaly? *Geophys Res Lett* 29(24):2232. <https://doi.org/10.1029/2002GL015243>
- Holliday NP, Hughes SL, Bacon S, Beszczynska-Möller A, Hansen B, Lavin A et al (2008) Reversal of the 1960s to 1990s freshening trend in the northeast North Atlantic and Nordic Seas. *Geophys Res Lett* 35(3):3614
- Hu S, Sprintall J (2016) Interannual variability of the Indonesian throughflow: the salinity effect. *J Geophys Res Oceans* 121:2596–2615
- Hu S, Sprintall J (2017) Observed strengthening of interbasin exchange via the Indonesian seas due to rainfall intensification. *Geophys Res Lett* 44(3):1448–1456
- Huang BY, Xue Y, Zhang DX, Kumar A, McPhaden MJ (2010) The NCEP GODAS ocean analysis of the tropical Pacific mixed layer heat budget on seasonal to interannual time scales. *J Clim* 23(18):4901–4925
- Huffman GJ, Adler RF, Bolvin DT, Gu G, Nelkin EJ, Bowman KP, Hong Y, Stocker EF, Wolff DB (2007) The TRMM multi-satellite precipitation analysis: quasi-global, multi-year, combined-sensor precipitation estimates at fine scale. *J Hydrometeorol* 8(1):38–55
- Krishnamurthy L, Krishnamurthy V (2014) Influence of PDO on south Asian summer monsoon and monsoon–ENSO relation. *Clim Dyn* 42(9–10):1–14
- Lau KM (2009) East Asian summer monsoon rainfall variability and climate teleconnection. *J Meteorol Soc Jpn* 70(1B):211–242
- Lee T, Fournier S, Gordon AL, Sprintall J (2019) Maritime Continent water cycle regulates low-latitude chokepoint of global ocean circulation. *Nat Commun* 10(1):2103. <https://doi.org/10.1038/s41467-019-10109-z>
- Li LRW, Schmitt C, Ummenhofer KK (2016a) North Atlantic salinity as a predictor of Sahel rainfall. *Sci Adv* 2:e1501588
- Li L, Schmitt RW, Ummenhofer C, Karnauskis K (2016b) Implications of North Atlantic Sea surface salinity for summer precipitation over the US Midwest: mechanisms and predictive value. *J Clim* 29:3143–3159
- Liu C, Wang D, Chen J, Du Y, Xie Q (2012a) Freshening of the intermediate water of the South China Sea between the 1960s and the 1980s. *Chin J Oceanol Limnol* 30(6):1010–1015
- Liu Q, Huang R, Wang D (2012b) Implication of the South China Sea throughflow for the interannual variability of the regional upper-ocean heat content. *Adv Atmos Sci* 29(1):54–62
- Lukas R, Lindstrom E (1991) The mixed layer of the western equatorial Pacific Ocean. *J Geophys Res Atmos* 96(S01):3343–3358
- Maes C, Picaut J, Belamari S (2002) Salinity barrier layer and onset of El Niño in a Pacific coupled model. *Geophys Res Lett* 29(24):591–594
- Maes C, Picaut J, Belamari S (2005) Importance of salinity barrier layer for the buildup of El Niño. *J Clim* 18:104–118
- Manabe S, Stouffer RJ (1995) Simulation of abrupt climate change induced by freshwater input to the north Atlantic Ocean. *Nature* 378(6553):165–167
- Menezes VV, Macdonald AM, Schatzman C (2017) Accelerated freshening of Antarctic Bottom Water over the last decade in the Southern Indian Ocean. *Sci Adv* 3:e1601426
- Michel S, Chapron B, Tournadre J, Reul N (2007) Sea surface salinity variability from a simplified mixed layer model of the global ocean. *Ocean Sci Discuss* 4(1):41–106
- Munk W (2003) Ocean freshening, sea level rising. *Science* 300(5628):2041–2043
- Nan F, Xue H, Chai F, Wang D, Yu F, Shi M, Guo P, Xiu P (2013) Weakening of the Kuroshio intrusion into the South China Sea over the past two decades. *J Clim* 26:8097–8110
- Nan F, Yu F, Xue H, Zeng L, Wang D, Yang S et al (2016) Freshening of the upper ocean in the South China Sea since the early 1990s. *Deep Sea Res Part I* 118:20–29
- Niiler PP, Kraus EB (1977) One-dimensional models of the upper ocean. In: Kraus EB (ed) *Modeling and prediction of the upper layers of the ocean*, vol 325. Pergamon, New York, pp 143–172
- Qu T, Du Y, Meyers G, Ishida A, Wang D (2005) Connecting the tropical Pacific with Indian Ocean through South China Sea. *Geophys Res Lett* 32:L24609. <https://doi.org/10.1029/2005GL024698>
- Qu T, Du Y, Sasaki H (2006) South China Sea throughflow: a heat and freshwater conveyor. *Geophys Res Lett* 33(23):430–452
- Ren L, Speer K, Chassignet EP (2011) The mixed layer salinity budget and sea ice in the Southern Ocean. *J Geophys Res* 116(C8):239–255
- Sarafanov A, Falina A, Sokov A, Demidov A (2008) Intense warming and salinification of intermediate waters of southern origin in the eastern subpolar North Atlantic in the 1990s to mid-2000s. *J Geophys Res* 113(C12):451–459
- Sasaki H, Nonaka M, Masumoto Y, Sasai Y, Uehara H, Sakuma H (2007) An eddy-resolving hindcast simulation of the quasi-global ocean from 1950 to 2003 on the Earth Simulator. In: Ohfuchi W, Hamilton K (eds) *High resolution numerical modeling of the atmosphere and ocean*. Springer, Berlin, pp 157–185

- Schmitt RW (1995) The ocean component of the global water cycle. U.S. National Report to International Union of Geodesy and Geophysics, 1991–1994, Supplement to Reviews of Geophysics, pp 1395–1409
- Schmitt RW (2008) Salinity and the global water cycle. *Oceanography* 21(1):12–19
- Schmitt RW, Blair A (2015) A River of Salt. *Oceanography* 28(1):40–45
- Skliris N, Marsh R, Josey SA, Good SA, Liu C, Allan RP (2014) Salinity changes in the world ocean since 1950 in relation to changing surface freshwater fluxes. *Clim Dyn* 43(3–4):709–736
- Song YT (2006) Estimation of interbasin transport using ocean bottom pressure: theory and model for Asian marginal seas. *J Geophys Res* 111:1119. <https://doi.org/10.1029/2005JC003189>
- Wang B, Zhang Y, Lu MM (2004) Definition of South China Sea monsoon onset and commencement of the east Asia summer monsoon. *J Clim* 17(4):699–710
- Wang D, Liu Q, Huang RX, Du Y, Qu T (2006) Interannual variability of the South China Sea throughflow inferred from wind data and an ocean data assimilation product. *Geophys Res Lett* 33(14):110–118
- Wijffels S, Schmitt R, Bryden H, Stigebrandt A (1992) Transport of freshwater by the oceans. *J Phys Oceanogr* 22:155–162
- Wong APS, Bindoff NL, Church JL (1999) Large-scale freshening of intermediate waters in the Pacific and Indian Oceans. *Nature* 400:440–443
- Wu P, Wood R, Stott P (2004) Does the recent freshening trend in the North Atlantic indicate a weakening thermohaline circulation? *Geophys Res Lett* 31(2):2301
- Xiu P, Chai F, Shi L, Xue HJ, Chao Y (2010) A census of eddy activities in the South China Sea during 1993–2007. *J Geophys Res* 115:C03012. <https://doi.org/10.1029/2009JC005657>
- Yang Y, Wang D, Wang Q, Zeng L, Xing T, He Y, Shu Y, Chen J, Wang Y (2019) Eddy-induced transport of saline Kuroshio water into the northern South China Sea. *J Geophys Res Oceans* 124:6673–6687
- Yaremchuk M, McCreary J Jr, Yu Z, Furue R (2009) The South China Sea throughflow retrieved from climatological data. *J Phys Oceanogr* 39:753–767
- Yu L (2015) Sea-surface salinity fronts and associated salinity-minimum zones in the tropical ocean. *J Geophys Res Oceans* 120(6):4205–4225
- Yu K, Qu T (2013) Imprint of the Pacific Decadal Oscillation on the South China Sea throughflow variability. *J Clim* 26(24):9797–9805
- Yu L, Weller RA (2007) Objectively analyzed air-sea heat fluxes for the global ice-free oceans (1981–2005). *Bull Am Meteorol Soc* 88:527–539
- Zeng L, Liu WT, Xue H, Xiu P, Wang D (2014) Freshening in the South China Sea during 2012 revealed by Aquarius and in situ data. *J Geophys Res Oceans* 119(12):8296–8314
- Zeng L, Wang D, Xiu P, Shu Y, Wang Q, Chen J (2016a) Decadal variation and trends in subsurface salinity from 1960 to 2012 in the northern South China Sea. *Geophys Res Lett* 43:12181–12189
- Zeng L, Wang D, Chen J, Wang W, Chen R (2016b) SCSPD14, a South China Sea physical oceanographic dataset derived from in situ measurements during 1919–2014. *Sci Data* 3:160029. <https://doi.org/10.1038/sdata.2016.29>
- Zeng L, Chassignet EP, Schmitt RW, Xu X, Wang D (2018) Salinification in the South China Sea since late 2012: a reversal of the freshening since the 1990s. *Geophys Res Lett* 45:2744–2751
- Zhao D, Wang W, Qin H, Mao Q, Wang D, Chen R (2014) Decadal changes of the intermediate water at 18°N in the South China Sea. *Acta Oceanol Sin (in Chinese)* 36(9):56–64

**Publisher's Note** Springer Nature remains neutral with regard to jurisdictional claims in published maps and institutional affiliations.